A Study of Tube Amplifier Modeling Using Nonlinear Wave Digital Filters

Matthias Hotz

Abstract—In recent years the simulation of vacuum-tube amplifiers, in particular guitar tube amplifiers, gained the attention of companies and the scientific community. One of the published approaches is based on nonlinear wave digital filters, which have the unique advantage of providing a structural relationship between the physical amplifier circuit and the digital model. In this article the theory behind nonlinear wave digital filters as well as a tube stage circuit is discussed thoroughly and on this basis a real-time capable wave digital model is derived. All necessary simplifications are highlighted and an improvement to the existing model is proposed and evaluated. Concluding, practical considerations regarding the accuracy and real-time capability are presented.

Index Terms—Vacuum Tube, Thermionic Valve, Amplifier, Modeling, Simulation, Virtual Analog, Wave Digital Filters, Nonlinear, Numerical Integration.

I. INTRODUCTION

AMPLIFIERS based on vacuum-tubes may seem highly antiquated, but even nowadays they are used as high fidelity audio amplifiers and instrument amplifiers and still many companies are developing and manufacturing such devices [1]. Especially in the realm of guitar amplifiers they are highly acclaimed, where the characteristic sound originating from the nonlinear behavior of overdriven vacuum-tube amplifiers was essential to the development of, e.g., blues and rock music. As those amplifiers exhibit some major disadvantages, including heavy weight, sensitivity to mechanical shocks, poor power efficiency, and most often a high price tag, the desire for an accurate simulation as a digital device emerged, in order to benefit from the advantages of digital systems and semiconductor technology. In the following, the simulation of a *guitar tube amplifier* is considered and thus *real-time capability* is a fundamental requirement, as the amplifier provides aural feedback to the artist.

Several approaches towards the modeling of tube amplifiers have been published [2], e.g., the combination of linear filters and waveshapers [3], nonlinear state-space models [4], [5] or the approximation of differential equations [6]. However, the method proposed by Karjalainen and Pakarinen [7]–[9] has one distinct advantage: it offers a *structural relationship* to the electrical circuit of the physical tube amplifier. Their approach, which will also be pursued here, is based on *wave digital filters* [10]. Originally, wave digital filters have been
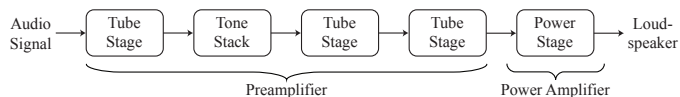
Fig. 1. Basic structure of a typical guitar tube amplifier, cf. [18].

developed for linear electrical networks comprising lumped elements which are discretized "element by element" and were later extended to include nonlinear elements [11], which are required to model the behavior of the vacuum-tube. It may be of interest to the reader that nonlinear wave digital filters already experienced frequent use for *physical modeling* in musical acoustics and sound generation [12]–[14], partly because their compatibility to *digital waveguide models* [15], [16] allows hybrid structures [17].

A complete tube amplifier is rather complex and may be viewed as a cascade of different blocks as depicted in Fig. 1. The modeling of the whole amplifier is out of scope of this work and thus only the main source of distortion, the *tube stage*, is considered. In the following an introduction to the necessary theory is given and subsequently, based on the work of Pakarinen and Karjalainen [9], a wave digital model is derived, where all necessary simplifications are discussed and an improvement of the model is proposed and evaluated. Finally, practical considerations are given and the accuracy and real-time capability of the model is highlighted.

II. WAVE DIGITAL FILTERS

A. Origination, Principle and Properties

Fettweis [19] noticed in the context of LC-ladder filters that the sensitivity to coefficient variations is much smaller if the filter is described by a special *system of differential equations* corresponding to the LC-ladder structure compared to a *single* differential equation describing the same transfer behavior. Consequently, a method to determine such systems of differential equations for *realizable* digital filters is desirable, as coefficient accuracy is inherently limited due to quantization. Realizability requires that the arithmetic operations can be ordered sequentially, which is equivalent to the requirement that every feedback loop of the digital filter's signal flow graph contains at least one delay element, i.e., it does not contain any *delay-free loops* [10], [19].

The most straightforward approach is to directly discretize the *linear* electrical circuit comprising lumped elements, called *reference filter*, using voltage v and current i, sometimes referred to as *Kirchhoff variables*, as signals. Correspondence between the continuous-time reference filter and the discrete-time filter must be established in the frequency domain, due
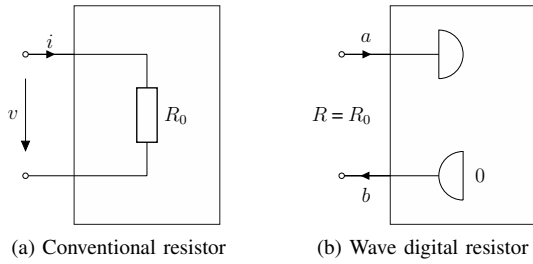
(a) Conventional resistor   (b) Wave digital resistor

Fig. 2. Transformation of a resistor: (a) depicts a lumped resistor and (b) the corresponding wave digital resistor, where ▷ denotes a *wave sink* and ◁ denotes a *wave source*. The connection comprising the incident wave a, reflected wave b and port resistance R is called *port*.

(a) Conventional capacitor   (b) Wave digital capacitor

Fig. 3. Transformation of a capacitor: (a) depicts a lumped capacitor and (b) the corresponding wave digital capacitor.

to the different time domain representations, and the mapping must be *nonlinear*, because an infinite frequency range is transformed to a finite one (*frequency warping*). Owing to its property of preserving *stability* and *passivity*, the *bilinear transform* [20], [21], i.e.,

$$s = \frac{2}{T}\left(\frac{1 - z^{-1}}{1 + z^{-1}}\right) , \qquad (1)$$

is chosen to relate the reference filter's s-plane of its system function (Laplace transform) to the z-plane of the discrete-time filter's system function (z-transform), with T being the *sampling period*. In the time domain the bilinear transform corresponds to numerical integration using the *trapezoidal rule*.[1],[2]

If the bilinear transform is applied to the Kirchhoff variables describing the electrical circuit, the resulting signal flow graph exhibits delay-free loops, as the elements, such as resistors and capacitors, as well as Kirchhoff's voltage and current law are characterized by a direct dependence between voltage and current. In order to circumvent this problem, Fettweis [10] introduced so-called *wave variables*, hence the name *wave digital filters* for the resulting structures. The wave variables are given by a transform of the Kirchhoff variables v and i with one degree of freedom and are reminiscent of the wave variables of microwave engineering (cf., e.g., [27]). Although different wave quantities may be used [28], only *voltage waves*, i.e.,

$$a = v + Ri \qquad\qquad b = v - Ri , \qquad (2)$$

are considered here,[3] where a is called the *incident wave*, b the *reflected wave* and the transform parameter R is called *port resistance*. If $R \neq 0$, the inverse transform

$$v = \frac{1}{2}\left(a + b\right) \qquad\qquad i = \frac{1}{2R}\left(a - b\right) \qquad (3)$$

exists and, therewith, the elements and Kirchhoff's laws can be transformed *individually* to the wave digital domain, where

[1]This is verified by comparing the transfer functions $H(s) = 1/s$ of a continuous-time integrator and $H(z) = T/2 \cdot (1 + z^{-1})/(1 - z^{-1})$ of a discrete-time integrator based on the trapezoidal rule of integration.

[2]Note that other numerical integration methods may be used to increase accuracy, e.g., as discussed in [22]–[26].

[3]Other types are current and power waves, where current waves lead to similar structures as voltage waves and power waves exhibit more multipliers in common adaptors but have certain advantages when the port resistance is time-varying [10], [28]–[30].
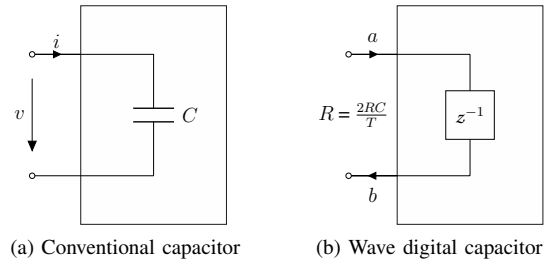
the port resistance is used to suppress delay-free loops as illustrated below. However, for validity of the properties of wave digital filters, all port resistances must be *positive* [10]. Before the discussion is continued with the transformation of elements, some key properties of wave digital filters shall be mentioned, i.e.,

- preservation of stability, passivity and, if present, loss-lessness of the reference filter [10], [31],
- low sensitivity w.r.t. coefficient quantization [10], [31],
- no granularity nor overflow limit cycles [10], [32],
- improvement of dynamic range and reduction of round-off noise by using appropriate structures [10], [33],
- suitability for time-varying filters [29], [34]–[36], and
- low computational complexity and real-time capability.

B. Elements

Elements like resistors and capacitors are transformed to the wave digital domain by expressing their underlying physical law in terms of wave variables, applying the bilinear transform, and finally choosing the port resistance such that *instantaneous reflection*, i.e., dependence of the current sample of the reflected wave on the current sample of the incident wave, is avoided. In the following, only subsequently required elements are derived, a more extensive range is presented for example in [10].

1) Resistor: A resistor R_0 as in Fig. 2a is described by Ohm's law

$$v = R_0 i ,$$

which is frequency-independent and thus a consideration of the time domain is sufficient. With (3), the relation is transformed to the wave digital domain, resulting in

$$b = \frac{R_0 - R}{R_0 + R}a .$$

Hence, by choosing the port resistance R as

$$R = R_0 ,$$

the reflected wave b becomes independent of the incident wave a, in particular

$$b = 0 ,$$

leading to the *wave digital resistor* in Fig. 2b.

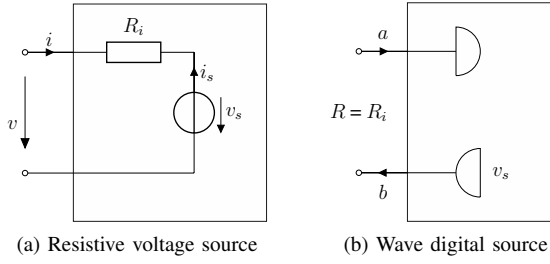(a) Resistive voltage source   (b) Wave digital source

Fig. 4.   Transformation of a resistive voltage source: (a) depicts the circuit and (b) the corresponding wave digital resistive voltage source.

2) Capacitor: A capacitor C as in Fig. 3a is described by

$$i = C\frac{\mathrm{d}v}{\mathrm{d}t}$$

and exhibits frequency-dependent behavior. Entering the wave domain using (3), taking the Laplace transform and applying the bilinear transform in (1) gives

$$B\left(1 + K\right) = A(1 - K) + z^{-1}\left[A\left(1 + K\right) - B\left(1 - K\right)\right] \ ,$$

with A and B being the z-transform of a and b, and

$$K = \frac{2RC}{T} \ .$$

Therefore, requiring

$$1 - K \overset{!}{=} 0$$

avoids instantaneous reflection, leading to the port resistance

$$R = \frac{T}{2C}$$

and the expression

$$B = z^{-1} A$$

for the reflected wave. Hence the reflected wave is the incident wave delayed by one sample. A graphical representation of the *wave digital capacitor* is depicted in Fig. 3b.

3) Resistive Voltage Source: An ideal voltage source inherently leads to instantaneous reflection (cf. [10], [19]) and is not applicable in the subsequently considered structure. However, the case is different for a voltage source with an internal resistance R_i as in Fig. 4a. Utilizing Kirchhoff's voltage and current law gives

$$v - R_i i = v_s \ ,$$

which, in conjunction with (3), develops to

$$b\left(R_i + R\right) = 2Rv_s + a\left(R_i - R\right)$$

in the wave domain. Choosing the port resistance as

$$R = R_i$$

suppresses instantaneous reflection and gives rise to the reflected wave

$$b = v_s \ .$$

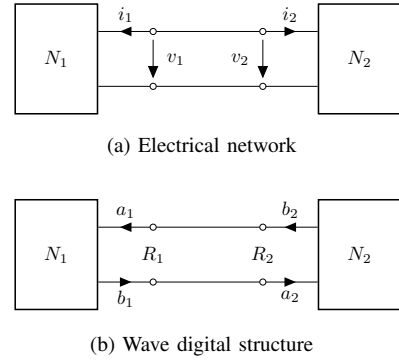The resulting *wave digital resistive voltage source* is illustrated in Fig. 4b.

(a) Electrical network

(b) Wave digital structure

Fig. 5.   Direct interconnection of two one-port elements N_1 and N_2: (a) electrical network and (b) the corresponding wave digital structure.

C. Adaptors

Adaptors manage the interconnection of elements under consideration of the topology [10], [37]. In order to develop an intuitive understanding for adaptors, the direct interconnection of two one-port elements N_1 and N_2 as shown in Fig. 5 shall be discussed. Kirchhoff's voltage and current law state the *continuity constraints* which must be met, i.e.,

$$v_1 = v_2 \qquad\qquad i_1 = -i_2 \ .$$

With (3), these constraints are given in terms of wave variables and solving for the reflected waves b_1 and b_2 yields (cf. [10])

$$b_1 = a_2 + \gamma(a_2 - a_1) \qquad b_2 = a_1 + \gamma(a_2 - a_1) \ ,$$

where

$$\gamma = \frac{R_1 - R_2}{R_1 + R_2} \ .$$

Therefore, two elements may only be connected directly if γ is zero, i.e., if both port resistances are *equal*. Otherwise some sort of *wave scattering* is necessary, as in this case the reflected waves are functions of both incident waves. Precisely this wave scattering is performed by an adaptor.

Subsequently, the series and parallel adaptor are described. Connections which are not decomposable to series and parallel connections require special consideration and are addressed, e.g., in [38].

1) Series Adaptor: For the series connection of N one-port elements, Kirchhoff's laws demand

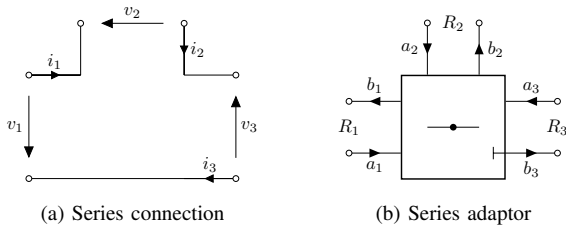$$v_1 + v_2 + \ldots + v_N = 0 \qquad i_1 = i_2 = \ldots = i_N \ .$$

In the same fashion as before, the reflected waves are derived with (3) as (cf. [10])

$$b_k = a_k - \gamma_k \sum_{i=1}^{N} a_i \ , \qquad\qquad k = 1, \ldots, N \qquad (4)$$
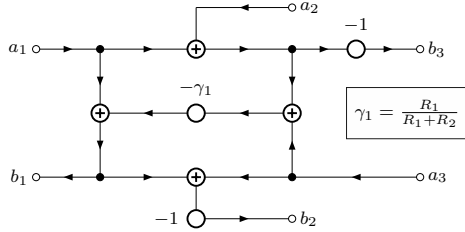
where

$$\gamma_k = \frac{2R_k}{\sum_{i=1}^{N} R_i} \ . \qquad\qquad (5)$$

Therewith, the behavior of the adaptor is fully described. However, two aspects deserve particular reference. First, adding up

(a) Series connection

(b) Series adaptor

(c) Signal flow diagram of the adaptor [10]

Fig. 6.   Series connection of three elements: (a) circuit topology, (b) three-port wave digital series adaptor where port 2 is the dependent port and port 3 is reflection-free, indicated by a ⊢ at its output, and (c) the corresponding signal flow diagram.

(a) Parallel connection

(b) Parallel adaptor
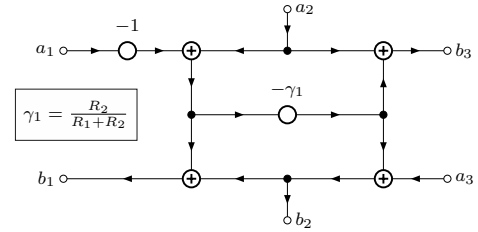
(c) Signal flow diagram of the adaptor [10]

Fig. 7.   Parallel connection of three elements: (a) circuit topology, (b) three-port wave digital parallel adaptor where port 2 is the dependent port and port 3 is reflection-free, and (c) the corresponding signal flow diagram.

all γ_k yields

$$\sum_{k=1}^{N} \gamma_k = 2 . \qquad (6)$$

This permits to express one coefficient γ_ν as a function of the $N-1$ remaining coefficients and the associated port ν is then called *dependent port*. The advantage thereof is a simplification of the computation [10], [37]. As to the second aspect, it is assumed that one port ν has an arbitrary port resistance R_ν. If this port resistance is chosen to be the sum of all other port resistances, i.e.,

$$R_\nu = \sum_{\substack{i=1 \\ i \neq \nu}}^{N} R_i , \qquad (7)$$

then (5) evaluates for its associated coefficient to $\gamma_\nu = 1$. Using this result in (4) yields

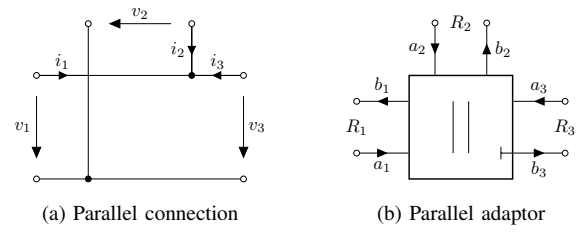$$b_\nu = -\sum_{\substack{i=1 \\ i \neq \nu}}^{N} a_i .$$

Consequently, the reflected wave b_ν is independent of the incident wave a_ν and the port ν is called *reflection-free*[4] [10], [37]. The benefit of a reflection-free port might not be immediately obvious, but subsequent sections will reveal its fundamental importance to wave digital filters.

Finally, Fig. 6 depicts a *three-port series adaptor*, where port 2 is the dependent port and port 3 is reflection-free.

2) Parallel Adaptor: For the parallel connection of N one-port elements, Kirchhoff's laws demand

$$v_1 = v_2 = \ldots = v_N \qquad i_1 + i_2 + \ldots + i_N = 0 .$$

[4]Note that only one port per adaptor may be reflection-free, because if a second coefficient is 1, then (6) implies a two-port adaptor where no wave scattering occurs.

Again, using (3) and solving for the reflected waves gives

$$b_k = -a_k + \sum_{i=1}^{N} \gamma_i a_i , \qquad k = 1, \ldots, N \qquad (8)$$

where, expressed in *port conductances* G_k,

$$\gamma_k = \frac{2G_k}{\sum_{i=1}^{N} G_i} , \qquad G_k = \frac{1}{R_k} . \qquad (9)$$

Analogous to the series adaptor, as (6) also holds for the coefficients in (9), a *dependent port* may be defined. Furthermore, if one port ν has an arbitrary port conductance G_ν and it is chosen to be the sum of all other port conductances, i.e.,

$$G_\nu = \sum_{\substack{i=1 \\ i \neq \nu}}^{N} G_i , \qquad (10)$$

then (9) evaluates for its associated coefficient to $\gamma_\nu = 1$ and, therewith, (8) yields

$$b_\nu = \sum_{\substack{i=1 \\ i \neq \nu}}^{N} \gamma_i a_i ,$$

i.e., a *reflection-free port*. Finally, Fig. 7 depicts a *three-port parallel adaptor*, where port 2 is the dependent port and port 3 is reflection-free.

D. Interconnection

When wave digital blocks are interconnected, some principles must be respected in order to arrive at valid and realizable structures [10]:

1) Blocks must be connected *port to port*, i.e., a pair of incident and reflected wave of one block is connected to *exactly one* pair of incident and reflected wave of another block.

2) When two ports are connected to each other, the *direction of wave flow* must be respected, i.e., the reflected wave terminal of one port is connected to the incident wave terminal of the other port.

3) Two ports may only be connected if their port resistances are *equal*.

4) There must not exist any *delay-free loop*[5].

Considering Section II-C, the first three requirements are plausible and easy to satisfy, but the fourth requirement has an extensive impact, mainly because of the behavior of adaptors. Both adaptors, series and parallel, exhibit a direct dependence of every reflected wave on every incident wave as visible in (4) and (8). If only elements without instantaneous reflection – including those presented in Section II-B – are connected to a *single* adaptor, no delay-free loops will emerge. However, more complex topologies require the interconnection of multiple adaptors, but due to the mentioned direct dependence of the reflected wave on the incident wave at a port of an adaptor this leads to delay-free loops. Fortunately, this statement does not consider that the port resistance of the connection between two adaptors is *arbitrary*, permitting a choice according to (7) or (10), causing *one* of the ports to become reflection-free. As the reflected wave of a reflection-free port does not depend on its incident wave, the delay-free loop is avoided.

Therewith a possibility was found to interconnect adaptors, and this implicates further consequences. As an arbitrary number of adaptors may be connected sequentially, an N-port adaptor can be realized by chaining $N - 2$ three-port adaptors [37]. Furthermore, in order to connect N adaptors, $N - 1$ reflection-free ports are required to avoid delay-free loops, provided that their interconnection does not form any loop, i.e., they are connected successively or in a tree-like manner. Consequently, as an adaptor has maximal one reflection-free port, only *one* of the N adaptors may have no reflection-free port and its choice implicates the position of the reflection-free port of all other adaptors.[6] This fact is essential when nonlinearities shall be included.

E. Nonlinearities

Wave digital filters as introduced above are limited to networks comprising only *linear* elements, because corresondence to the reference filter is established via the frequency domain. However, seen from a different point of view, the wave digital methodology is a *numerical solver* for the dynamic system described by the reference filter using the trapezoidal rule for numerical integration [30]. Thus, if the laws of the analog domain, the occurance of exclusively positive port resistances and the numerical integration method are respected, nonlinear elements may be included as well, but the interpretation of the trapezoidal rule as bilinear transform is *not* valid anymore [30]. In the following, *memoryless* nonlinearities, i.e., nonlinear resistors, are discussed, whereas nonlinearities with memory,
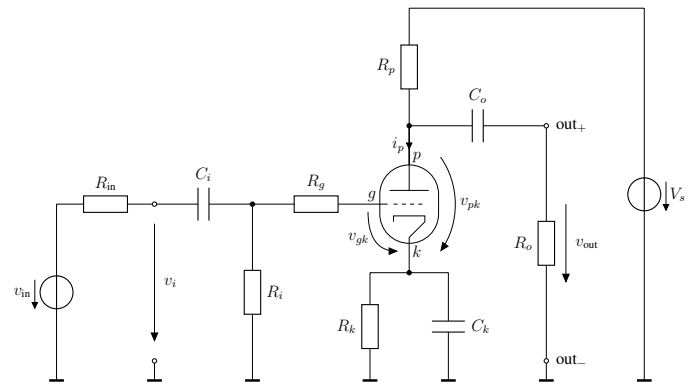
Fig. 8. Tube stage circuit [9], where v_{in} is the input voltage signal and the output voltage v_{out} is tapped at R_o.

in particular algebraic nonlinearities [39], are addressed, e.g., in [40]–[42].

A nonlinear resistor is characterized by a *signal-dependent* relationship between voltage and current, hence the relationship in the wave domain is also signal-dependent. Consequently, a fixed port resistance is not sufficient to suppress direct dependence of the reflected wave on the incident wave and, therefore, nonlinear resistors always exhibit instantaneous reflection. As pointed out in Section II-D, the reflected waves of adaptors depend directly on the incident waves, thus simply connecting a nonlinear resistor to an adaptor leads to a delay-free loop. The only way to circumvent this problem is to connect the nonlinear resistor to a reflection-free port, but therewith the number of nonlinear resistors in structures like those considered at the end of Section II-D is *limited to one*, because all other reflection-free ports are required for the interconnection of adaptors.[7] Due to reasons discussed in the previous section, the reflection-free ports of all other adaptors will be oriented towards the adaptor to which the nonlinearity is connected, giving rise to a tree-like structure for which systematic and efficient methods for the implementation exist [44].

Besides the limitation to one nonlinearity, there are limitations on the memoryless nonlinearity itself as well. In particular, when the nonlinearity is transformed to the wave domain, the mapping from an incident wave to a reflected wave must be *unique* as otherwise ambiguities emerge [11]. Furthermore, it might be impossible to derive an explicit solution for the reflected wave, resulting in an *implicit equation* which must be solved using an *iterative algorithm* as, e.g., the Newton-Raphson method. Such an iterative algorithm might prohibit real-time execution, requiring the use of *look-up tables* [7] or other means [45].

III. Modeling of a Tube Preamplifier Stage

A. Tube Stage

Tube stages typically comprise a common-cathode circuit similar to the one depicted in Fig. 8, where the input voltage

---

[5]For a more formal definition see Section IV-A and Theorem 1 in [10].

[6]Note that this statement is valid if one-port elements as the ones in Section II-B are used, but is not generally valid if elements with two or more ports are included.

[7]However, there are means to include multiple nonlinearities, see for example [12], [43].
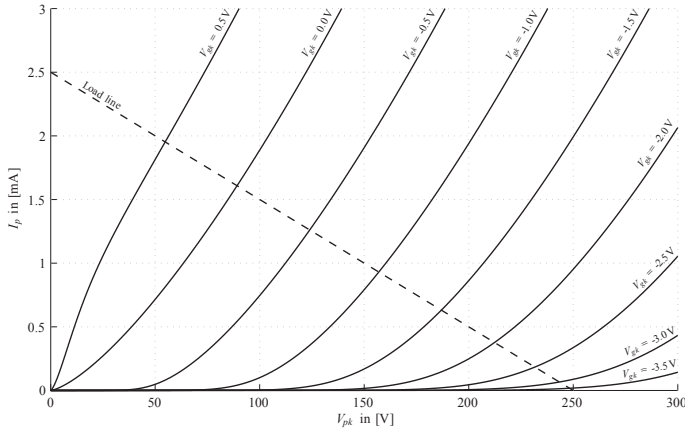
Fig. 9. Characteristic curves of the triode tube 12AX7, approximated by the model in (11). The intersection of the load line with the characteristic curves gives the actual plate current I_p assuming a plate resistor $R_p = 100\,\mathrm{k\Omega}$ and a supply voltage $V_s = 250\,\mathrm{V}$, with the cathode connected directly to ground for design purposes. This assists in the choice of the operating point for a best possible linear amplification.

signal v_{in} appears amplified, phase-inverted, and possibly distorted as output voltage v_{out}. In the following, the component values

$$R_{\mathrm{in}} = 1\,\Omega \qquad R_k = 1\,\mathrm{k\Omega} \qquad C_i = 100\,\mathrm{nF}$$
$$R_i = 1\,\mathrm{M\Omega} \qquad R_p = 100\,\mathrm{k\Omega} \qquad C_k = 10\,\mu\mathrm{F}$$
$$R_g = 20\,\mathrm{k\Omega} \qquad R_o = 1\,\mathrm{M\Omega} \qquad C_o = 10\,\mathrm{nF}$$

and a supply voltage of $V_s = 250\,\mathrm{V}$ as in [9] are used. Before the wave digital modeling of this tube stage circuit is discussed, its central element, the tube, as well as some aspects regarding the operation and occurring phenomena shall be highlighted.

1) Vacuum-Tube: Tube stages commonly feature a *triode tube* having the terminals *grid* g, *plate* p, and *cathode* k. The basic functionality may be described as an electron flow from the cathode to the plate established by the plate-to-cathode voltage v_{pk}, whose flow rate is controlled by the grid-to-cathode voltage v_{gk} as it, if negative, "pushes back" electrons towards the cathode. However, this is a utmost rudimentary view on the operation and a more elaborate discussion of the physical principles of vacuum-tubes can be found, e.g., in [46].

In order to simulate the behavior of a tube, a model which is compatible with circuit theory must be found. The prevailing approach is to use a current source for the plate current i_p, which is controlled by v_{gk} and v_{pk}. For this relationship several physically informed models like the Child-Langmuir law or [47]–[51] exist. Still, due to its improved fit to actual tube characteristics, the model of Koren [52] based on the phenomenological equation

$$i_p = \frac{v_1^{k_x}}{k_{g1}}\left(1 + \mathrm{sgn}\left(v_1\right)\right)\ , \tag{11}$$

where

$$v_1 = \frac{v_{pk}}{k_p}\log\left(1 + \exp\left(k_p\left(\frac{1}{\mu} + \frac{v_{gk}}{\sqrt{k_{vb} + v_{pk}^2}}\right)\right)\right)\ ,$$
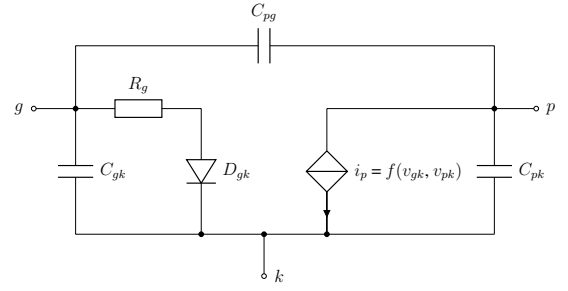

Fig. 10. Equivalent circuit for a triode tube as proposed by Koren.[8]

is utilized. Furthermore, Koren provides the parameters for various tubes [52], including those for the triode tube *12AX7*,

$$k_x = 1.4 \qquad k_{g1} = 1060 \qquad k_p = 600$$
$$\mu = 100 \qquad k_{vb} = 300\ .$$

The 12AX7 is equivalent to the European tube *ECC83* and commonly used in tube stages and adopted here as well. Its characteristics, approximated by the tube model of Koren, are depicted in Fig. 9. Up to now, only the path from plate to cathode was considered, but a complete model requires all paths to be respected. Based on the physical background, the plate and grid are assumed to be mutually insulated. However, the case is different for the path from grid to cathode. If v_{gk} is negative, electrons are repelled from the grid and no current flow from grid to cathode is observed, i.e., the connection has high resistance. Though, if v_{gk} is positive, electrons are attracted and a current between grid and cathode starts to flow. This behavior is reminiscent of a diode and may be modeled as such. Concluding, a fairly accurate equivalent circuit for a triode tube is shown in Fig. 10, which corresponds to the SPICE model published by Koren[8] and includes *parasitic capacitances* arising from the physical arrangement.

2) Principle of Operation: In the following, the tube stage circuit in Fig. 8 is briefly discussed. More detailed information is found, e.g., in [53], [54].

a) Grid circuit: The grid circuit consists of C_i, being a coupling capacitor, R_i, which ties the grid with high resistance to ground, and R_g, whose function is to limit the grid current if v_{gk} becomes positive. Thus, if an input voltage v_i drives the tube stage, only its AC component appears at the grid.

b) Cathode circuit: As can be seen in Fig. 9, if v_{gk} varies around $-1\,\mathrm{V}$, the change in plate current is maximally linear and, thus, this is a suitable bias voltage to define the operating point. Instead of applying a negative DC offset to the grid, it is common practice to lift the potential of the cathode, which is realized by the cathode circuit comprising R_k and C_k. R_k is selected so that the quiescent current causes the desired DC offset and C_k stabilizes the voltage, which would otherwise vary at the rate of the input signal.

c) Plate circuit: The plate circuit, consisting of R_p, C_o and R_o, is the load of the tube. Its impedance is domiated by R_p, whereas C_o is a coupling capacitor and R_o is used to tap the output voltage.

(a) Tube stage circuit
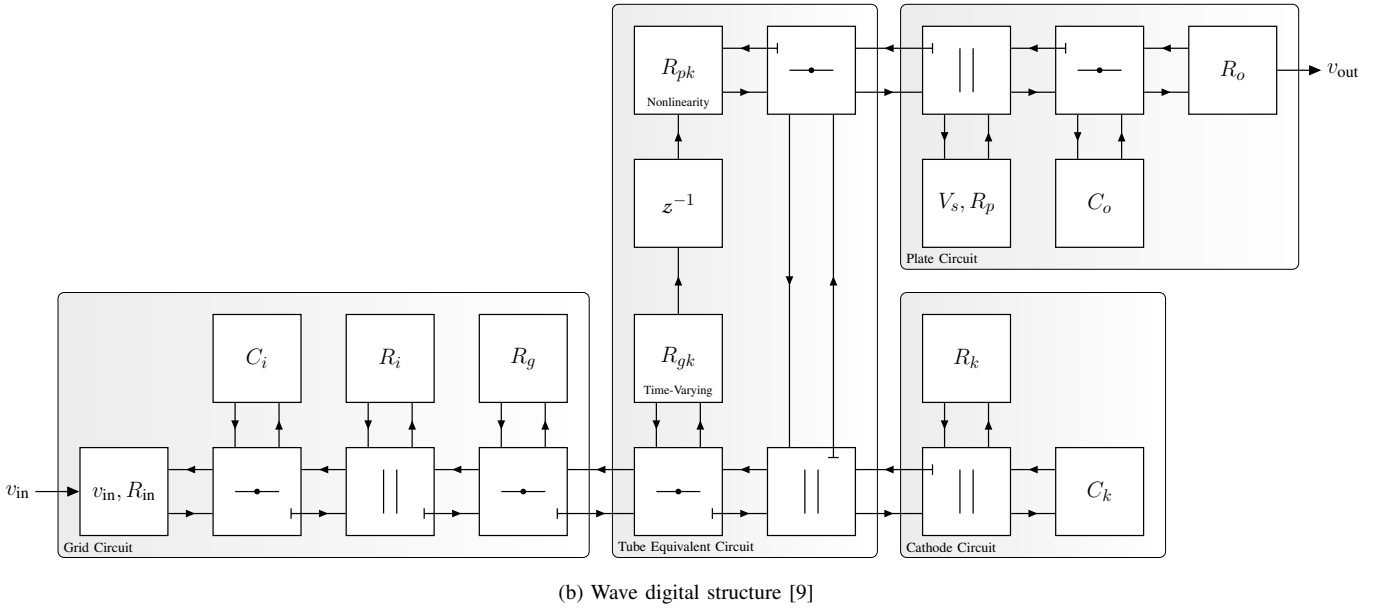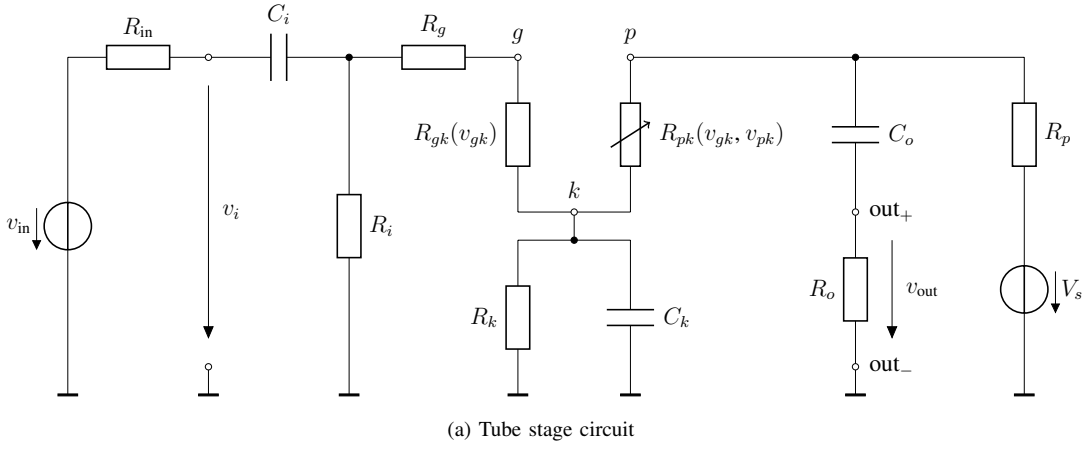

(b) Wave digital structure [9]

Fig. 11.   Derivation of the wave digital model of the tube stage: (a) tube stage circuit with a simplified triode tube model, and (b) the corresponding wave digital structure, where the behavior of D_{gk} is specified in (12).

3) Sound-Shaping Phenomena: Concluding the discussion of the tube stage, the phenomena having the most influence on the sound shall be pointed out [2]. Clearly, the nonlinear behavior of the plate current in (11) is the primary source of signal distortion, but for large input signals, which force v_{gk} to become positive, the diode between grid and cathode introduces distortion as well. Furthermore, the grid current emerging for positive v_{gk} charges the input capacitor C_i, involving a shift of the operating point and causing *blocking distortion* [9], [55]. Regarding the cathode circuit, as the cathode current varies at the rate of the input signal and the low-pass consisting of R_k and C_k can not completely remove the AC component, a *feedback* to the input occurs. Finally, the parasitic capacitances of the tube depicted in Fig. 10 involve additional filtering, where the *Miller effect* [53] deserves a special notice.

B. Wave Digital Model

In order to derive a wave digital model of the tube stage, the limitations of nonlinear wave digital filters must be considered.

Regarding the topology, the tube stage circuit in Fig. 8 is rather simple and characterized by exhibiting only series and parallel connections of elements, thus the adaptors presented in Section II-C suffice. Unfortunately, this is not valid for the tube equivalent circuit in Fig. 10, where C_{pg} leads to a Δ-connection of the three terminals. The constraint on the topology is met by a simplification of the tube equivalent circuit, in particular by not taking into account the parasitic capacitances, assuming that their influence is minor at audio frequencies. However, another issue emerges as the tube equivalent circuit involves *two* nonlinearities, the controlled current source and the diode, but as discussed in Section II-E the structure is limited to one. Although it is possible to represent the tube as a three-port nonlinearity, which combines both nonlinearities into one, this option will not be considered as it is too complex for practical implementations. The approach introduced in [9] is to represent the grid-to-cathode path as a "switched resistor,"

$$R_{gk}(v_{gk}) = \begin{cases} R_{gk,c} = 2.7\text{k}\Omega & \text{for } v_{gk} > 0 \\ R_{gk,b} = 100\text{G}\Omega & \text{else ,} \end{cases} \qquad (12)$$

which reduces the number of nonlinearities to one, at the price of a coarse approximation and making the wave digital structure time-varying. Furthermore, as the state depends on v_{gk} and, due to the change of resistance, v_{gk} depends on the state, an iterative evaluation is necessary which prohibits real-time application. Pakarinen and Karjalainen [9] circumvented this problem by using the previous sample of v_{gk} to determine the state of R_{gk}. However, this is an intrusion on the system's dynamics and leads to errors. As the state is determined by a decision boundary at $v_{gk} = 0$, one might assume that extrapolation would probably predict v_{gk} on the correct side of the decision border and therefore lead to the correct state. Consequently, a linear extrapolation of $\tilde{v}_{gk}[n]$ based on the two previous samples, i.e.,

$$\tilde{v}_{gk}[n] = 2v_{gk}[n-1] - v_{gk}[n-2] \,, \tag{13}$$

is proposed for state determination. Regarding the plate-to-cathode path, interpreting (11) as the defining equation for a nonlinear resistor $R_{pk}(v_{gk}, v_{pk})$ is more appropriate with respect to the wave digital domain, as then the considerations of Section II-E apply. A closer look at (11) reveals that there is a similar problem as in the case of R_{gk}, because R_{pk} depends on v_{gk}, which is not "local" to the resistor and thus extends the impact of the implicit equation from the resistor itself to a sub-circuit of the tube stage. Again, Pakarinen and Karjalainen [9] proposed to use the previous sample of v_{gk}, which leads to the fact that the plate current i_p is delayed by one sample and, consequently, also the output voltage and its influence on the cathode potential, degrading the feedback. However, extrapolation is not advisable in this case, as the extrapolation error manifests itself directly on the model output.

Summarizing, if the simplified tube equivalent circuit is inserted into Fig. 8, the circuit in Fig. 11a results, which permits a transformation into the wave digital domain. Thus, if the theory of Section II is applied, the wave digital structure depicted in Fig. 11b is obtained, where in favor of readability the port resistances were omitted. Note that due to Principle 3 of Section II-D, an adaptor inherits the port resistances of the elements connected to it and, therewith, the adaptor's coefficient γ_1 and the port resistance of the reflection-free port is specified. If the elements are not *time-varying*, those values are fixed, but if there is a time-varying element as in the case of R_{gk}, they need to be updated every time the element and, therewith, its port resistance changes. Furthermore, through the reflection-free ports this change affects all adaptors on the path to the nonlinearity and even has impact on the nonlinearity itself, as the port resistance of its associated adaptor's port changes. During the discussion of R_{gk}, the idea of an improved approximation using more resistors may come to mind, but as every state change involves such an update, the number of resistors is limited in practical implementations. Concluding, the expression obtained for the nonlinear resistor R_{pk}, if (11) is transformed to the wave digital domain using (3), is rather complex and prohibits an explicit solution for the reflected wave. Hence, the resulting implicit equation needs to be solved, where a real-time model probably necessitates a look-up table with precalculated results.[9]

IV. RESULTS AND DISCUSSION

A. Implementation and Method of Evaluation

The wave digital model in Fig. 11b was implemented using Simulink 7.5 of MathWorks. In order to evaluate its accuracy and correctness, a reference model based on the tube circuit in Fig. 8, with the simplified tube model expained in Section III-B, was implemented using the non-real-time circuit simulator LTSpice IV.[10] The input voltage sources of both models were controlled by samples of a 24-bit/44.1 kHz WAVE file and the output voltages were recorded in the same format, hence the sampling period of the wave digital model was set to

$$T = \frac{1}{44.1\,\text{kHz}} \,.$$

The WAVE files of the output voltages served for the comparison of the models. As a measure of similarity, two characteristic values are presented, the *mean squared error* of the output voltage of the wave digital model with respect to the output voltage of the reference model, i.e.,

$$\text{MSE} = \left\langle (v_{\text{out,WD}} - v_{\text{out,LTSpice}})^2 \right\rangle \,,$$

where $\langle \cdot \rangle$ denotes the *empirical mean*, and a *signal-to-noise ratio* defined as

$$\text{SNR} = 10\log\left(\frac{\overline{P}_{\text{ref}}}{\text{MSE}}\right) \,,$$

where $\overline{P}_{\text{ref}}$ is the mean power of the reference model output voltage produced at $1\,\Omega$, i.e.,

$$\overline{P}_{\text{ref}} = \left\langle v_{\text{out,LTSpice}}^2 \right\rangle \,.$$

B. Stimulation with Small Amplitude Sinusoid

Fig. 12 shows the simulation outcome if the tube stage is driven by a $1\,\text{kHz}$-sinusoid of $1\,\text{V}$ amplitude. The output voltages of both models match very well, in particular

$$\text{MSE} = 6.0\,\text{mV}^2 \qquad \text{SNR} = 53.5\,\text{dB} \,.$$

The input signal amplitude is small, thus the sinusoid at the output is basically undistorted and R_{gk} stays in the blocking state throughout. However, the impact on the dynamics of R_{pk} by using a delayed version of v_{gk} as discussed in Section III-B prohibits an exact consistency with the reference model due to the modified feedback to the grid circuit. Noteworthy is also the transient effect visible at the beginning, which can be attributed to the initial charging of the capacitors.

C. Stimulation with Large Amplitude Sinusoid

In order to force a change of R_{gk}'s state and, therewith, allow a comparison of the two different approaches for state

---

[9]Note that the look-up table is two-dimensional, but a separate look-up table is required for every state of R_{gk}, due to its influence on the port resistance seen by the nonlinearity.

[10]All solver-related parameters were set to the default values, except "Default Integration Method" was changed to "trapezoidal".
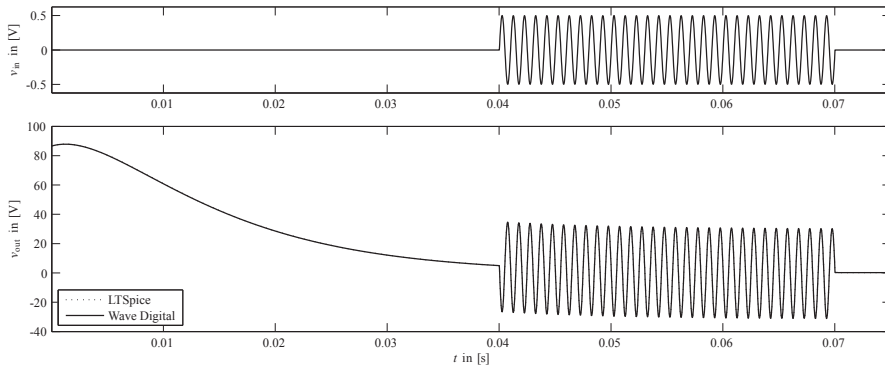
Fig. 12. Stimulation of the tube stage with a 1 kHz sinusoid having an amplitude of 0.5 V. The upper diagram depicts the input voltage signal and the lower diagram the output of the wave digital model as well as the LTSpice reference model. The output voltages are nearly the same and, therefore, visually indistinguishable.
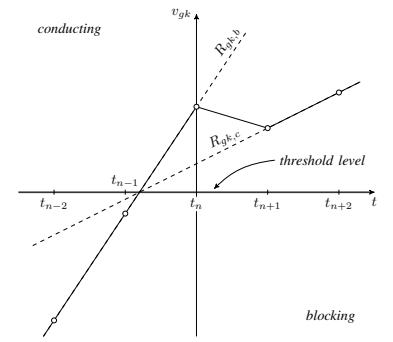
Fig. 13. Voltage v_{gk} over R_{gk} in (12) if the state is determined using $v_{gk}[n-1]$ and a linearly increasing current is applied. Owing to the delayed state change a "glitch" occurs.

(a) Output voltage if R_{gk}'s state is based on $v_{gk}[n-1]$

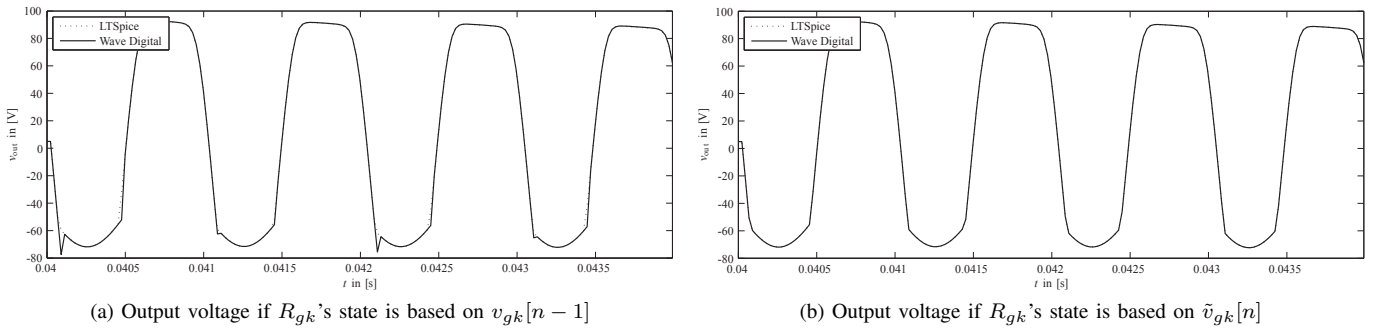(b) Output voltage if R_{gk}'s state is based on $\tilde{v}_{gk}[n]$

Fig. 14. Stimulation of the tube stage with a 1 kHz sinusoid having an amplitude of 3 V, where only an excerpt is shown to improve the visibility of the occurring effects: output voltage of the wave digital model with R_{gk}'s state determined by (a) the previous sample $v_{gk}[n-1]$ and (b) the linear extrapolation $\tilde{v}_{gk}[n]$ defined in (13).

determination discussed in Section III-B, the tube stage is driven with a sinusoid as in the previous example, but with an amplitude of 3 V, causing v_{gk} to become positive. First, the model determining the state of R_{gk} based on the previous sample $v_{gk}[n-1]$ as proposed by [9] shall be discussed, whose output is depicted in Fig. 14a. The impact on the system's dynamics takes its toll, degrading the accuracy to

$$\text{MSE} = 1932.7\,\text{mV}^2 \qquad \text{SNR} = 32.0\,\text{dB}$$

due to a systematic deviation from the reference model. For a better understanding thereof, the state change is illustrated for a specific setup in Fig. 13, showing that the deviation is inherent to that approach.

In contrast, Fig. 14b depicts the output voltage of the model determining the state of R_{gk} using the linear extrapolation $\tilde{v}_{gk}[n]$ defined in (13). The state of R_{gk} is successfully predicted and thus a good performance is achieved, namely

$$\text{MSE} = 13.7\,\text{mV}^2 \qquad \text{SNR} = 53.5\,\text{dB}\ .$$

A comparison to the other approach attests a definitive advantage, but the method also has two drawbacks. On one hand, the extrapolation only works well if the signal frequency is low compared to the sampling frequency. However, in a practical scenario this issue is relativized due to reasons discussed in the next section. On the other hand, in a particular case a *state oscillation* was observed, which may appear if v_{gk} is close to zero for more than one sample. Unfortunately, there was not

enough time for a deeper analysis thereof and thus must be left as future work.

### D. Stimulation with High-Frequency Sinusoid

The final example considers a 5 kHz[11] sinusoid driving the tube stage, where the amplitude is large enough to force state changes of R_{gk}. After the transient effect vanished, excerpts of the output signals were extracted and the magnitude spectra were calculated using a fast Fourier transform (FFT), whose results are depicted in Fig. 15a and 15b for the LTSpice reference model and the wave digital model with the R_{gk} state determination via linear extrapolation, respectively. The reference model shows the fundamental wave at about 5 kHz and the harmonics introduced by the nonlinearity are also clearly visible. Furthermore, aliasing effects corrupt the output signal, as high-frequency harmonics are folded back into the base band, recognizable by the various peaks beside the ones at multiples of 5 kHz. Turning the look towards the output of the wave digital model gives a disastrous view. The cause thereof is that the state of R_{gk} is often incorrect, which severely corrupts the output signal.

As indicated by the output of the reference model, a practical implementation would require oversampling to reduce

---

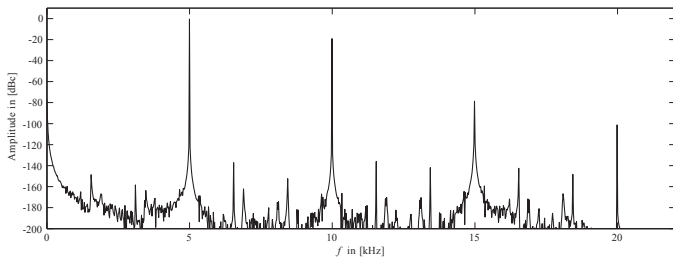[11]The signal frequency is actually $(232/2048) \cdot 44.1\,\text{kHz} \approx 4.996\,\text{kHz}$ in order to reduce the leakage effect when a 2048-point FFT with a rectangular window is applied, but to avoid an unnecessary complication of the text it will be referred to as 5 kHz.
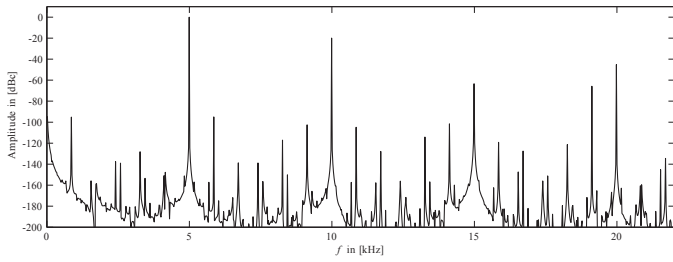
(a) Magnitude response of the reference model
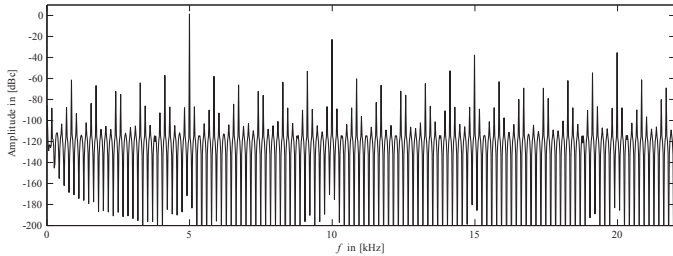
(b) Magnitude response of the wave digital model

(c) Magnitude response of the wave digital model with 4 times oversampling

Fig. 15.   Stimulation of the tube stage with a 5 kHz sinusoid having an amplitude of 3 V. After the transient effect vanished, excerpts of the output signals were extracted to derive the magnitude responses shown above.

the aliasing effects [9]. Fortunately, this also increases the accuracy of the linear extrapolation of v_{gk} as a side effect, leading to an improvement of the state prediction. This fact is shown in Fig. 15c, where the input signal was first upsampled by a factor of 4, then applied to the wave digital model running with a sampling period of

$$T = \frac{1}{4 \times 44.1 \, \text{kHz}}$$

and the obtained output signal was low-pass filtered and downsampled again. Concluding, as oversampling is already required to avoid aliasing effects, the state prediction based on linear extrapolation of v_{gk} is also adequate for input signals with high-frequency content.

E. Computational Requirements

The simulation of the wave digital model in Simulink was unexpectedly slow, which can probably be attributed to the fact that the implicit equation of the nonlinearity was solved iteratively for every sample. This gave the impulse to perform a coarse estimation of the number of arithmetic operations, which are to be expected for a real-time implementation. With the details provided in Section II, the number of arithmetic operations for all blocks in Fig. 11b except R_{pk} may be determined. Assuming that R_{pk} is realized as a two-dimensional

look-up table with bilinear interpolation and that the structure is precomputed for both states of R_{gk} so that a state change reduces to memory operations (cf. Section III-B), one arrives at about 90 arithmetic operations per output sample. Although this may just be seen as a "order of magnitude"-kind of value, it already indicates that the computational requirements of this model are rather moderate.

V. Conclusion

The thorough discussion of the theory made the necessity for simplifications evident to arrive at a real-time capable model. The limitations of nonlinear wave digital filters required the omission of the parasitic capacitances of the tube as well as an approximation of the tube's diode-like behavior of the grid-to-cathode path, a reasonable compromise, though. Furthermore, two intrusions into the system's dynamics were necessary to achieve real-time capability, leading to a deviation from the reference model. Nevertheless, considering the proposed improvement, these deviations are minor and may be tolerated in a practical implementation, especially if the benefit of low computational requirements is kept in mind.

The wave digital model of the tube stage as well as some audio samples are provided on the website of the Signal Processing and Speech Communication Laboratory[12] at Graz University of Technology. An aural evaluation of the model based on the audio samples may lead to the conclusion, at least in the opinion of the author, that the fundamental character of the achieved distortion is decent, but raw and unshaped. This leads back to the introduction, where the scope was discussed. For a sonically pleasing simulation it is not sufficient to consider only a part of the amplifier, instead the cascading of tube stages, the tone stack [56], power amplifier, output transformer [8], [57], [58] and the loudspeaker [59] must be taken into account as well, as every element contributes its part to the whole picture – and this, as Pakarinen and Karjalainen [9] put it, remains a challenging future task.

VI. Acknowledgments

References

[1] E. Barbour, "The cool sound of tubes," *IEEE Spectrum*, vol. 35, no. 8, pp. 24 –35, Aug. 1998.

[2] J. Pakarinen and D. T. Yeh, "A review of digital techniques for modeling vacuum-tube guitar amplifiers," *Computer Music J.*, vol. 33, pp. 85–100, Jun. 2009.

[3] U. Zölzer, Ed., *DAFx: Digital Audio Effects*.   New York, NY, USA: John Wiley & Sons, Inc., 2002.

[4] D. T. Yeh and J. O. Smith, "Simulating guitar distortion circuits using wave digital and nonlinear state-space formulations," *Proc. 11th Int. Conf. Digital Audio Effects (DAFx-08)*, Sep. 2008.

[5] I. Cohen and T. Helie, "Real-time simulation of a guitar power amplifier," *Proc. 13th Int. Conf. Digital Audio Effects (DAFx-10)*, Sep. 2010.

[6] J. Macak and J. Schimmel, "Real-time guitar tube amplifier simulation using an approximation of differential equations," *Proc. 13th Int. Conf. Digital Audio Effects (DAFx-10)*, Sep. 2010.

[12]http://www.spsc.tugraz.at/student_projects/nl-wdf-amp-sim

[7] M. Karjalainen and J. Pakarinen, "Wave digital simulation of a vacuum-tube amplifier," in *Proc. IEEE Int. Conf. Acoustics, Speech and Signal Processing (ICASSP 2006)*, vol. 5, May 2006, pp. 153–156.

[8] J. Pakarinen, M. Tikander, and M. Karjalainen, "Wave digital modeling of the output chain of a vacuum-tube amplifier," *Proc. 12th Int. Conf. Digital Audio Effects (DAFx-09)*, pp. 55–59, Sep. 2009.

[9] J. Pakarinen and M. Karjalainen, "Enhanced wave digital triode model for real-time tube amplifier emulation," *IEEE Trans. Audio, Speech, and Language Processing*, vol. 18, no. 4, pp. 738–746, May 2010.

[10] A. Fettweis, "Wave digital filters: Theory and practice," *Proc. IEEE*, vol. 74, no. 2, pp. 270–327, Feb. 1986.

[11] K. Meerkötter and R. Scholz, "Digital simulation of nonlinear circuits by wave digital filter principles," in *Proc. IEEE Int. Symp. Circuits and Systems*, vol. 1, May 1989, pp. 720–723.

[12] G. De Sanctis and A. Sarti, "Virtual analog modeling in the wave-digital domain," *IEEE Trans. Audio, Speech, and Language Processing*, vol. 18, no. 4, pp. 715–727, May 2010.

[13] R. Rabenstein, S. Petrausch, A. Sarti, G. De Sanctis, C. Erkut, and M. Karjalainen, "Blocked-based physical modeling for digital sound synthesis," *IEEE Signal Processing Magazine*, vol. 24, no. 2, pp. 42–54, Mar. 2007.

[14] F. Pedersini, A. Sarti, and S. Tubaro, "Object-based sound synthesis for virtual environments using musical acoustics," *IEEE Signal Processing Magazine*, vol. 17, no. 6, pp. 37–51, Nov. 2000.

[15] J. O. Smith, "Principles of digital waveguide models of musical instruments," in *Applications of Digital Signal Processing to Audio and Acoustics*, ser. The Kluwer Int. Series in Engineering and Computer Science, M. Kahrs and K. Brandenburg, Eds. Springer, 2002, vol. 437, pp. 417–466.

[16] ——, *Physical Audio Signal Processing*. http://ccrma.stanford.edu/~jos/pasp/, accessed May 10, 2011, online book.

[17] M. Karjalainen, "Blockcompiler: Efficient simulation of acoustic and audio systems," in *Audio Engineering Society Conv. 114*, Mar. 2003.

[18] H. Lemme, *Gitarren-Verstärker Sound*. München, Germany: Pflaum Verlag, 1995.

[19] A. Fettweis, "Digital filter structures related to classical filter networks," in *Selected Papers in Digital Signal Processing*, D. S. P. Committee, Ed. IEEE PRESS, 1975, vol. II, pp. 475–485.

[20] A. V. Oppenheim and R. W. Schafer, *Discrete-Time Signal Processing*, 3rd ed. Upper Saddle River, NJ, USA: Prentice Hall Press, 2009.

[21] J. G. Proakis and D. K. Manolakis, *Digital Signal Processing – Principles, Algorithms, and Applications*, 4th ed. New Jersey, USA: Pearson Prentice Hall, 2007.

[22] K. Ochs, "Passive integration methods: Fundamental theory," *AEU - Int. J. Electronics and Communications*, vol. 55, no. 3, pp. 153 – 163, 2001.

[23] D. Fränken and K. Ochs, "Numerical stability properties of passive runge-kutta methods," in *Proc. IEEE Int. Symp. Circuits and Systems (ISCAS 2001)*, vol. 3, May 2001, pp. 473 –476 vol. 2.

[24] ——, "Synthesis and design of passive runge-kutta methods," *AEU - Int. J. Electronics and Communications*, vol. 55, no. 6, pp. 417 – 425, 2001.

[25] ——, "Improving wave digital simulation by extrapolation techniques," *AEU - Int. J. Electronics and Communications*, vol. 56, no. 5, pp. 327 – 336, 2002.

[26] ——, "Automatic step-size control in wave digital simulation using passive numerical integration methods," *AEU - Int. J. Electronics and Communications*, vol. 58, no. 6, pp. 391 – 401, 2004.

[27] D. M. Pozar, *Microwave Engineering*, 3rd ed. John Wiley & Sons, Inc., 2004.

[28] G. Kubin, "Wave digital filters: Voltage, current, or power waves?" in *IEEE Int. Conf. Acoustics, Speech, and Signal Processing (ICASSP 1985)*, vol. 10, Apr. 1985, pp. 69–72.

[29] ——, "On the stability of wave digital filters with time-varying coefficients," in *European Conf. Circuit Theory and Design*, Prague, Czechoslovakia, Sep. 1985, pp. 499–502.

[30] S. Bilbao, *Wave and Scattering Methods for Numerical Simulation*. John Wiley & Sons, Ltd, 2004.

[31] A. Fettweis, "Pseudo-passivity, sensitivity, and stability of wave digital filters," *IEEE Trans. Circuit Theory*, vol. 19, no. 6, pp. 668–673, Nov. 1972.

[32] A. Fettweis and K. Meerkötter, "Suppression of parasitic oscillations in wave digital filters," *IEEE Trans. Circuits and Systems*, vol. 22, no. 3, pp. 239–246, Mar. 1975.

[33] A. Fettweis, "On sensitivity and roundoff noise in wave digital filters," *IEEE Trans. Acoustics, Speech and Signal Processing*, vol. 22, no. 5, pp. 383–384, Oct. 1974.

[34] H. W. Strube, "Time-varying wave digital filters for modeling analog systems," *IEEE Trans. Acoustics, Speech and Signal Processing*, vol. 30, no. 6, pp. 864–868, Dec. 1982.

[35] ——, "Time-varying wave digital filters and vocal-tract models," in *IEEE Int. Conf. Acoustics, Speech, and Signal Processing (ICASSP 1982)*, vol. 7, May 1982, pp. 923–926.

[36] S. Bilbao, "Time-varying generalizations of all-pass filters," *IEEE Signal Processing Letters*, vol. 12, no. 5, pp. 376–379, May 2005.

[37] A. Fettweis and K. Meerkötter, "On adaptors for wave digital filters," *IEEE Trans. Acoustics, Speech and Signal Processing*, vol. 23, no. 6, pp. 516–525, Dec. 1975.

[38] D. Fränken, J. Ochs, and K. Ochs, "Generation of wave digital structures for networks containing multiport elements," *IEEE Trans. Circuits and Systems I: Regular Papers*, vol. 52, no. 3, pp. 586–596, Mar. 2005.

[39] L. O. Chua, "Nonlinear circuits," *IEEE Trans. Circuits and Systems*, vol. 31, no. 1, pp. 69–87, Jan. 1984.

[40] T. Felderhoff, "A new wave description for nonlinear elements," in *IEEE Int. Symp. Circuits and Systems (ISCAS 1996)*, vol. 3, May 1996, pp. 221–224.

[41] A. Sarti and G. De Poli, "Generalized adaptors with memory for nonlinear wave digital structures," in *Proc. 8th European Signal Processing Conf. (EUSIPCO-96)*, vol. 3, Trieste, Italy, Sep. 1996, pp. 1941–1944.

[42] ——, "Toward nonlinear wave digital filters," *IEEE Trans. Signal Processing*, vol. 47, no. 6, pp. 1654–1668, Jun. 1999.

[43] S. Petrausch and R. Rabenstein, "Wave digital filters with multiple nonlinearities," in *Proc. 12th European Signal Processing Conf. (EUSIPCO-2004)*, Sep. 2004, pp. 77–80.

[44] A. Sarti and G. De Sanctis, "Systematic methods for the implementation of nonlinear wave-digital structures," *IEEE Trans. Circuits and Systems I: Regular Papers*, vol. 56, no. 2, pp. 460–472, Feb. 2009.

[45] D. Fränken, "Wave digital simulation of electrical networks containing nonlinear dynamical elements – a new approach," in *Proc. IEEE Int. Symp. Circuits and Systems (ISCAS 2000)*, vol. 1, May 2000, pp. 535–538.

[46] K. R. Spangenberg, *Vacuum Tubes*. New York, USA: McGraw-Hill Book Company, Inc., 1948.

[47] W. M. Leach, Jr., "SPICE models for vacuum-tube amplifiers," *J. Audio Engineering Society*, vol. 43, no. 3, pp. 117–126, 1995.

[48] E. K. Pritchard, W. M. Leach, Jr., F. Broydé, E. Clavelier, C. Hymowitz, and C. Rydel, "Comments on 'SPICE models for vacuum-tube amplifiers' and author's replies," *J. Audio Engineering Society*, vol. 45, no. 6, pp. 488–496, 1997.

[49] S. Reynolds, "Vacuum tube models for PSPICE simulations," *Glass Audio*, vol. 5, no. 4, 1993.

[50] C. Rydel, "Simulation of electron tubes with SPICE," in *Audio Engineering Society Conv. 98*, 2 1995.

[51] W. Sjursen, "Improved SPICE model for triode vacuum tubes," *J. Audio Engineering Society*, vol. 45, no. 12, pp. 1082–1088, 1997.

[52] N. L. Koren, "Improved vacuum tube models for SPICE simulations," *Glass Audio*, vol. 8, no. 5, pp. 18–27, 1996, available: http://www.normankoren.com/Audio/Tubemodspice_article.html, accessed May 11, 2011.

[53] F. Langford-Smith, Ed., *Radiotron Designer's Handbook*, 4th ed. Sydney, Australia: Wireless Press, 1953, available: http://www.ax84.com/rdh4.html, accessed June 26, 2011.

[54] R. Kuehnel, *Vacuum Tube Circuit Design: Guitar Amplifier Preamps*, 2nd ed. Seattle, WA, USA: Amp Books LLC, 2009.

[55] R. Aiken, "What is "blocking" distortion?" Internet Article, Jul. 2006, http://www.aikenamps.com/BlockingDistortion.html, accessed May 11, 2011.

[56] D. T. Yeh and J. O. Smith, "Discretization of the '59 Fender Bassman tone stack," *Proc. 9th Int. Conf. Digital Audio Effects (DAFx-06)*, Sep. 2006.

[57] R. C. D. de Paiva, J. Pakarinen, V. Välimäki, and M. Tikander, "Real-time audio transformer emulation for virtual tube amplifiers," *EURASIP J. Advances in Signal Processing*, vol. 2011, 2011.

[58] J. H. Chan, A. Vladimirescu, X.-C. Gao, P. Liebmann, and J. Valainis, "Nonlinear transformer model for circuit simulation," *IEEE Trans. Computer-Aided Design of Integrated Circuits and Systems*, vol. 10, no. 4, pp. 476–482, Apr. 1991.

[59] D. T. Yeh, B. Bank, and M. Karjalainen, "Nonlinear modeling of a guitar loudspeaker cabinet," *Proc. 11th Int. Conf. Digital Audio Effects (DAFx-08)*, pp. 89–96, Sep. 2008.